

# Optical waveguide characterization of a tristable antiferroelectric liquid crystal cell

S. A. Jewell<sup>a)</sup> and J. R. Sambles

*Thin Film Photonics Group, School of Physics, University of Exeter, EX4 4QL, United Kingdom*

J. W. Goodby, A. W. Hall, and S. J. Cowling

*Department of Chemistry, University of Hull, Kingston Upon Hull, HU6 7RX, United Kingdom*

(Received 14 August 2003; accepted 14 December 2003)

The optical convergent-beam waveguide technique has been used to characterize a homogeneously aligned 3  $\mu\text{m}$  cell containing a liquid crystal in the antiferroelectric phase. The director structure has been quantified with the cell at 0 V and at  $\pm 50$  V dc, and three distinct states have been observed. From the optical data collected, it is found that the material forms a tilted-bookshelf ferroelectric structure in the presence of a suitable voltage, and the characteristic alternating (anticlinic) structure of the antiferroelectric phase when the cell is short-circuited. The biaxiality of the antiferroelectric state has been measured, and (approximately) uniaxial refractive indices, the cone angle, and layer tilt have been determined for the ferroelectric state. © 2004 American Institute of Physics.

[DOI: 10.1063/1.1645972]

## INTRODUCTION

Antiferroelectric (AF) liquid crystals (LCs) are tilted, chiral, and smectic in nature and have great potential for use in display applications. They offer the same fast switching properties as conventional ferroelectric displays, but have the added advantage of three stable states. This results in a range of possible applications including improved gray-scale generation in displays and fast optical switches in the communications industry.

When a thin layer ( $<5 \mu\text{m}$ ) of AF LC is confined between two homogeneously aligning substrates, provided that the cell thickness is thinner than that of the natural pitch of the material, the natural helix is suppressed and a layered structure forms, with the tilt in alternating layers varying by  $180^\circ$  [Fig. 1(a)]. Each of the layers has a spontaneous polarization associated with it, the direction of which is parallel to the layer and normal to the primary director, with the direction of polarization alternating between the layers.<sup>1-3</sup> On the application of a sufficient dc field, coupling between the external field and the spontaneous polarization causes the director to uniformly align, producing a ferroelectric structure. This property therefore gives rise to two possible ferroelectric states [Figs. 1(b) and 1(c)], with the orientation being determined by the direction of the applied electric field. Switching between these two states causes the director to rotate around the surface of a cone, and it is this cone angle that determines the relative orientation of the primary director in the two applied voltage states. The result is that the optic axis differs in direction among all three cases, and hence the three states possess different optical properties.

Optical techniques have been used with great success for many years to probe LC cells and have yielded a wealth of information about the director structure in a wide range of

nematic and smectic materials.<sup>4-7</sup> The latest characterization method developed is the convergent-beam technique, which has previously been used to study the dynamics of LC cells in detail.<sup>8-11</sup> This method, which involves the collection of optical intensity versus angle-of-incidence data in the sub-millisecond timescale, is also ideally suited to studying the effect of applied voltages on an AF-filled cell, as it minimizes the amount of time that high voltages need to be applied to the cell while the data is being collected, reducing any risk of ionic decomposition of the material.

By measuring the optical properties of an AF cell in all three stable states, a wealth of detailed information, including the optical biaxiality, director alignment, layer structure, and cone angle of the material, can be obtained.

## EXPERIMENT

A 3  $\mu\text{m}$  cell was constructed from ITO-coated low-index glass ( $n = 1.52$ ) substrates. A homogeneously aligning polymer (JSR AL 1254) was spun down and baked onto both substrates. One substrate was then buffed with a velvet cloth to induce directed homogeneous alignment, while the other was left unbuffed (Fig. 2). The cell was then assembled using 3  $\mu\text{m}$  beads in a UV setting glue as spacers, and was filled by capillary action with the LC material (AH56, Hull) in the isotropic phase at  $95^\circ\text{C}$  and then slowly cooled into the AF phase with +50 V dc held across the cell to produce a good monodomain.

The cell was shorted, index matched between two low-index glass hemispheres, and enclosed in an insulating oven to allow a temperature of  $74.9^\circ\text{C}$  to be maintained. The rubbed polyimide surface was used as the incident face, with the rubbing direction parallel to the  $y$  axis (i.e.,  $0^\circ$  azimuth). This arrangement was then mounted at the center of an optical convergent-beam system (Fig. 3). Diffused light from a 35 mW HeNe laser ( $\lambda = 632.8 \text{ nm}$ ) was focused down onto the cell, and optical intensity versus angle-of-incidence data were collected for polarization, conserving and converting

<sup>a)</sup>Electronic mail: s.a.jewell@exeter.ac.uk

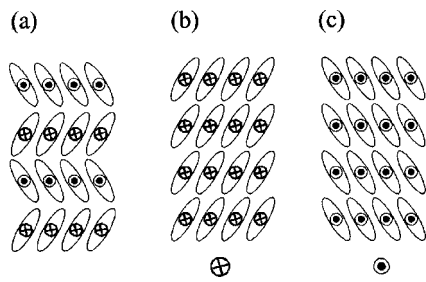


FIG. 1. (a) The layer structure in an AF cell at 0 V viewed along the layer normal, showing the alternating nature of the orientation of the spontaneous polarization in adjacent layers. (b) and (c) The ferroelectric layer structure formed when dc voltages of  $\pm 50$  V are applied to the cell.

signals from both incident *p*-polarized (transverse magnetic) and *s*-polarized (transverse electric) light. This was then repeated with dc voltages of +50 V and then -50 V applied across the cell. The data were then normalized and compared to model data generated using a multilayer optics modeling routine based on a 4×4 Berreman model.<sup>12</sup> The optical permittivity, absorption, and thickness of each of the layers, in addition to the director profile of the LC layer, were used as fitting parameters, and the best fit was determined by using a least-squares fitting procedure.

**RESULTS AND DISCUSSION**

Figure 4 shows a selection of optical intensity versus angle-of-incidence data collected for the three applied voltages (+50, -50, and 0 V). The clear differences among the optical data for the three voltages indicate that the director structure differs in each case. In particular, at the applied voltages, a critical-edge-type feature can clearly be seen at 76° angle of incidence in the  $T_{pp}$  and  $R_{pp}$  data, but this is not evident at 0 V. This indicates that the apparent optical permittivities for the material at both applied voltages are very similar (although the director structure clearly differs) and that the associated optical permittivity at 0 V is clearly different.

To obtain the director structure in the two applied voltage cases, the LC was approximated as a parallel aligned slab of a uniaxial material, with the azimuthal orientation of the director varying between the two voltages. Due to the high voltages applied and the negative dielectric anisotropy of the material, it was assumed that the director in both cases would be lying approximately parallel to the substrate (i.e., director tilt  $\theta \approx 90^\circ$ ). During the fitting procedure, the optical

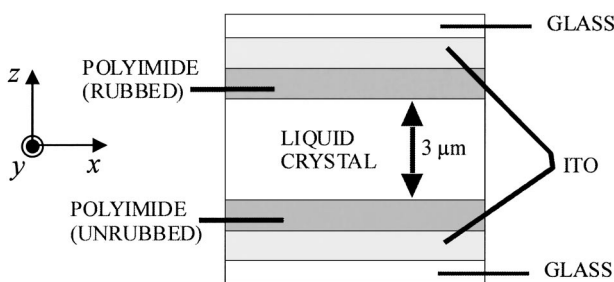


FIG. 2. Schematic diagram of a typical AF-filled LC cell.

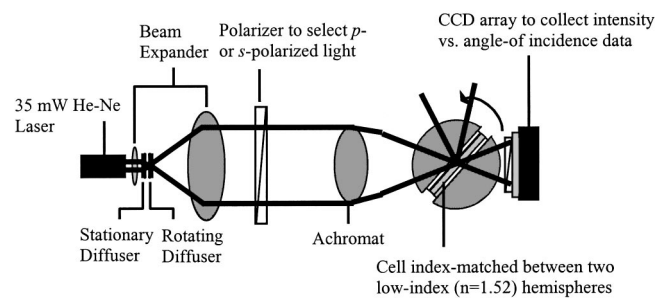


FIG. 3. Schematic diagram of the optical convergent-beam experiment.

permittivities, absorption, and thickness of the ITO and polyimide aligning layers were also allowed to vary, along with those of the LC. The optical data collected for the two voltages were fitted independently, and good agreement was found between the optical parameters determined for both cases. The two measured LC permittivities  $\epsilon_x$  and  $\epsilon_y$  (corresponding, respectively, to the ordinary and extraordinary permittivities in the uniaxial case), azimuthal angle  $\phi$  (measured from the *y* axis) and director tilt  $\theta$  (measured from the layer normal) for the two voltages are shown in Table I, and a selection of the final fits to the data is given in Fig. 4. The result is that for both voltages, the director lies approximately parallel to the substrate with an angle of 73.2° between the two measured azimuths.

The alternating-layer structure (anticlinic) in the 0 V AF state results in a more complex optical situation, requiring the optical biaxiality of the liquid crystal to be taken into consideration in the model. The alternating tilt in adjacent layers results in an effective dielectric tensor, which is the average of the dielectric tensors associated with the two types of layer alignment. The resulting dielectric tensor has optical permittivities, measured in the applied voltage (ferro-aligned) state ( $\epsilon_x$  and  $\epsilon_y$ ), related to those associated with the index-ellipsoid of the AF aligned state ( $\epsilon_1$ ,  $\epsilon_2$ , and  $\epsilon_3$ ) by the cone angle of the material.<sup>13</sup>

$$\epsilon_{AF} = \begin{pmatrix} \epsilon_x \cos^2 \theta + \epsilon_z \sin^2 \theta & 0 & 0 \\ 0 & \epsilon_y & 0 \\ 0 & 0 & \epsilon_x \sin^2 \theta + \epsilon_z \cos^2 \theta \end{pmatrix}. \tag{1}$$

Therefore, the three optical permittivities measured in the 0 V state correspond to<sup>1</sup>

$$\epsilon_1 = \epsilon_x \cos^2 \theta + \epsilon_z \sin^2 \theta, \tag{2}$$

$$\epsilon_2 = \epsilon_y, \tag{3}$$

$$\epsilon_3 = \epsilon_x \sin^2 \theta + \epsilon_z \cos^2 \theta. \tag{4}$$

In this case, for any cone angle other than 45°, the resulting optical tensor is biaxial, with the optic axis along  $\epsilon_2$  and collinear with the cone axis (for a 45° cone angle,  $\epsilon_x = \epsilon_y$ , so that the material would appear to be uniaxial). Initial attempts to fit the optical data for the 0 V case using the uniaxial multilayer fitting routine as employed in the applied voltage case were unsuccessful, indicating that the cone angle was not 45°. A biaxial code was then used to fit to the data, with the same uniaxial non-LC layer parameters as

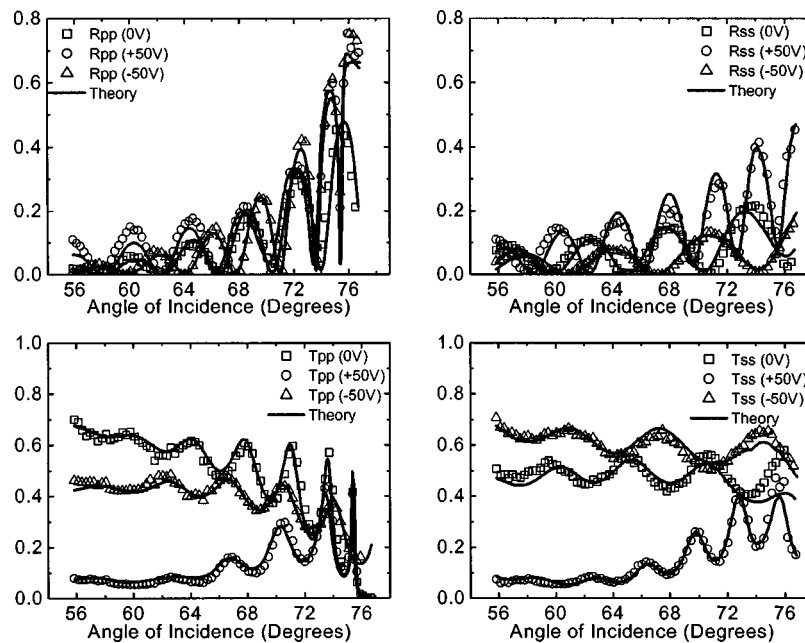


FIG. 4. Measured (symbols) and modeled (solid line) optical intensity versus angle-of-incidence data for the polarization conserving case ( $p$ - to  $p$ - and  $s$ - to  $s$ -) collected in reflection and transmission for the 0, +50, and -50 V states.

used in the applied voltage case. A reasonable result was achieved by approximating the cell as a uniformly aligned slab, with the orientation of the index ellipsoid described by the Euler angles given in Table I, and the resulting fit shown in Fig. 4. Although the quality of the fit is generally good, poor agreement is found between data and theory at the higher angles of incidence. This suggests that, although the uniformly aligned slab approximation is valid for the bulk of the cell, the alignment in regions close to the surfaces, which light at close to grazing incidence is particularly sensitive to, is more complex. Surface influences may also explain why the rubbing direction and the azimuthal orientation of the director at 0 V (which also coincides with the midpoint between the azimuths of the applied voltage cases) differ by  $\approx 27^\circ$ .

Using the optical permittivity  $\epsilon_1$  measured for the 0 V case and the values of  $\epsilon_x$  and  $\epsilon_z$  determined by fitting to the applied voltage data, in conjunction with Eq. (2), the cone angle of the material is calculated as  $\theta_c = 35.3 (\pm 0.1)^\circ$ . Similarly, using the measured value of  $\epsilon_3$  with Eq. (4) gives  $\theta_c = 36.4 (\pm 0.1)^\circ$ . Measurements made on the material us-

ing optical microscopy while switching a  $5 \mu\text{m}$  cell with a field of  $15 \text{ V } \mu\text{m}^{-1}$  gave the cone angle as  $35.6 (\pm 0.2)^\circ$ , which is in excellent agreement with the cone angles calculated here. Furthermore, adding together Eqs. (2) and (4) gives

$$\epsilon_1 + \epsilon_3 = \epsilon_x + \epsilon_z, \quad (5)$$

and from the measured values,  $\epsilon_1 + \epsilon_3 = 4.875 (\pm 0.004)$  and  $\epsilon_x + \epsilon_z = 4.881 (\pm 0.004)$ , again in excellent agreement.

The measured cone angle can be verified further by considering the geometry of the cone and tilted layers in the applied voltage case (Fig. 5). As stated previously, the Euler tilt angle measured at 0 V corresponds to the orientation of the axis of the cone, and hence the tilt angle  $\delta$  of the layer

TABLE I. Values for the real part of the optical permittivity of AH56 produced by performing a least-squares fitting procedure on the optical intensity versus angle-of-incidence data collected at applied voltages of  $\pm 50$  V dc, and at 0 V with the cell shorted. The Euler angles  $\phi$  (azimuthal twist) and  $\theta$  (director tilt) used to define the director orientation are also given.

	$\epsilon_x$ ( $\pm 0.001$ )	$\epsilon_y$ ( $\pm 0.001$ )	$\epsilon_z$ ( $\pm 0.001$ )	$\phi_F$ ( $\pm 0.1$ ) $^\circ$	$\theta_F$ ( $\pm 0.1$ ) $^\circ$
+50 V	2.166	2.166	2.719	9.1	93.2
-50 V	2.168	2.168	2.709	-64.1	89.0
0 V	$\epsilon_1$ ( $\pm 0.001$ )	$\epsilon_2$ ( $\pm 0.001$ )	$\epsilon_3$ ( $\pm 0.001$ )	$\phi_{AF}$ ( $\pm 0.1$ ) $^\circ$	$\theta_{AF}$ ( $\pm 0.1$ ) $^\circ$
	2.350	2.235	2.525	-27.4	-4.7

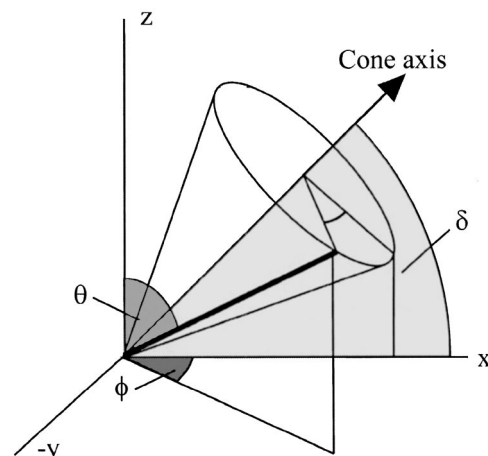


FIG. 5. Diagram to show the relationship between the director-azimuth ( $\phi$ ), director-tilt ( $\theta$ ), layer-tilt ( $\delta$ ), and cone-axis angles, where the cone axis is lying in the  $x$ - $z$  plane.

normal. This is related to the angle measured between the azimuths of the applied voltage and 0 V cases, and the director tilt angle  $\theta$  by the expression<sup>14</sup>

$$\cos(\theta_c) = \sin(\phi)\cos(\delta)\sin(\theta) + \sin(\delta)\cos(\theta). \quad (6)$$

The azimuthal angle  $\phi$  is the Euler angle twist, measured in the coordinate geometry where the cone axis lies in the  $x-z$  plane. Therefore, from the Euler angles measured in the +50 V case, the value of  $\phi$  is given by  $\phi = \phi_F - \phi_{AF} = 36.6^\circ$ . Here,  $\phi_F$  is the azimuthal twist of the applied voltage case and  $\phi_{AF}$  is that of the 0 V case. Using  $\delta = \theta_{AF} = -4.7^\circ$  (the measured tilt at 0 V and  $\theta = \theta_F = 93.2^\circ$  (the measured tilt at +50 V), Eq. (6) gives the cone angle as  $36.5^\circ$ , which is in excellent agreement with the values calculated by considering the biaxiality of the cell.

## CONCLUSIONS

The optical convergent-beam technique has been used to study the director alignment in the three stable states of an anticlinic antiferroelectric liquid crystal cell. The results show that, to a first approximation, when confined to a homogeneously aligned geometry, the material formed a tilted-bookshelf structure, with a layer tilt of  $-4.7^\circ$ . On the application of  $\pm 50$  V, two different ferroelectric structures form. In both cases, the director is aligned approximately parallel to the substrate, with the azimuthal orientation of the two states differing by  $73.2^\circ$ . At 0 V, the material formed layers

of alternating tilt, resulting in a more complex optical structure. By measuring the apparent permittivities in the 0 V state and using them in conjunction with those measured when the voltages were applied, the cone angle of the material was calculated as  $35.9^\circ \pm 0.6^\circ$ . This is in close agreement with the cone angle calculated by considering the orientation of the director at an applied voltage with respect to the layer normal, and also with optical measurements made on a cell switching at a high voltage.

- <sup>1</sup>G. Scalia, P. Rudquist, D. Herman, K. D'Have, S. T. Lagerwall, and J. R. Sambles, *J. Appl. Phys.* **91**, 9667 (2002).
- <sup>2</sup>K. D'Have, A. Dahlgren, P. Rudquist, J. P. F. Lagerwall, G. Andersson, M. Matuszczyk, S. T. Lagerwall, R. Dabrowski, and W. Drzewinski, *Ferroelectrics* **244**, 1 (2000).
- <sup>3</sup>L. A. Parry-Jones, S. M. Beldon, D. Rodriguez-Martin, R. M. Richardson, and S. J. Elston, *Liq. Cryst.* **29**, 8 (2002).
- <sup>4</sup>F. Z. Yang and J. R. Sambles, *J. Opt. Soc. Am. B* **16**, 3 (1999).
- <sup>5</sup>B. T. Hallam, F. Yang, and J. R. Sambles, *Liq. Cryst.* **26**, 5 (1999).
- <sup>6</sup>F. Yang, L. Ruan, and J. R. Sambles, *J. Appl. Phys.* **88**, 11 (2000).
- <sup>7</sup>S. A. Jewell and J. R. Sambles, *J. Appl. Phys.* **92**, 1 (2002).
- <sup>8</sup>S. A. Jewell and J. R. Sambles, *Appl. Phys. Lett.* **82**, 19 (2003).
- <sup>9</sup>L. Ruan and J. R. Sambles, *Phys. Rev. Lett.* **90**, 168701 (2003).
- <sup>10</sup>N. J. Smith, J. R. Sambles, and M. D. Tillin, *Phys. Rev. Lett.* **88**, 088301 (2002).
- <sup>11</sup>L. Ruan and J. R. Sambles, *J. Appl. Phys.* **92**, 4857 (2002).
- <sup>12</sup>D. Y. K. Ko and J. R. Sambles, *J. Opt. Soc. Am. A* **5**, 1863 (1988).
- <sup>13</sup>K. D'Have, P. Rudquist, S. T. Lagerwall, H. Pauwels, W. Drzewinski, and R. Dabrowski, *Appl. Phys. Lett.* **76**, 3528 (2000).
- <sup>14</sup>J. C. Jones and E. P. Raynes, *Liq. Cryst.* **11**, 199 (1992).